Rheological Modeling of the Tensile Creep Behavior of Paper

A. DeMaio, T. Patterson

Institute of Paper Science and Technology, Georgia Institute of Technology, Atlanta, Georgia

Received 7 August 2006; accepted 27 April 2007
DOI 10.1002/app.26895
Published online 28 August 2007 in Wiley InterScience (www.interscience.wiley.com).

ABSTRACT: Paper is a networked structure of randomly bonded fibers. These fibers are composed of naturally occurring polymeric materials (cellulose, hemicelluloses, and lignin). Polymeric materials such as these exhibit viscoelastic deformation, and as a result, creep under an applied stress. A rheological model has been developed to predict the tensile creep behavior of paper under a uniaxial stress. Specifically, the focus of this model was to predict creep strain using only stress, time, and efficiency factor (effectiveness of bonding). This rheological model offers insight into creep behavior (drawing from molecular creep mechanisms) and separates total strain from creep into initial elastic, primary creep, and secondary creep components. Interfiber bonding is taken into account through the use of an efficiency factor which represents how effectively bonding is distributing load throughout the fiber network of the paper. As a result, this model makes it possible to predict the creep behavior of paper over a range of bonding levels, induced by mechanical changes in bonded area or chemical modification of specific bond strength, using creep data from paper at any single level of bonding. This utility is retained as long as the fibers and the orientation of the fibers are not changed. © 2007 Wiley Periodicals, Inc. J Appl Polym Sci 106: 3543–3554, 2007

Key words: creep; tension; rheology; cellulose fibers; semicrystalline polymers

INTRODUCTION

In this article a rheological model of tensile creep in paper is developed. This model requires an initial experimental data set that is used to determine seven material constants. The constants characterize the elastic deformation, primary creep, and secondary creep properties of the paper. Given these constants the model predicts the strain of the paper for any level of internal bonding, initial applied load, or duration of loading greater than 10 s, assuming the fiber type has not been changed. It allows the magnitude of elastic deformation, primary creep, and secondary creep to be determined.

Paper is a complex structure composed of a network of bonded fibers. The fibers from softwood and hardwood trees, the primary fibers used for papermaking, are composed of natural polymers consisting of cellulose, hemicelluloses, and lignin.[1–4] Cellulose is a polysaccharide of β-D Glucopyranose and is a linear chain molecule.[1–3] In its naturally occurring form, between 50 and 70% of the cellulose polymer has a crystalline form, while the remainder has an amorphous arrangement.[1] Hemicelluloses are also polysaccharides, and are composed of combinations of monosaccharides, which include β-D Mannopyranose, β-D Galactopyranose, and β-D xylopyranose.[1] Hemicelluloses have a linear backbone, possess branches, have a lower degree of polymerization than cellulose[1–3] and are amorphous in nature.[4] Lignin is a highly branched amorphous polymer composed of phenylpropane units, coniferyl alcohol and sinapyl alcohol.[1]

Within a wood fiber, cellulose is arranged in tightly packed strands known as microfibrils.[3] Deposits of hemicelluloses and lignin surround these microfibrils forming a matrix.[3] This composite material is arranged in layers within a fiber.[3] These layers are the primary wall and the secondary wall. The secondary wall consists of three sublayers (S_1, S_2, and S_3). In the primary wall, cellulose microfibrils are arranged randomly.[3] In the secondary wall layers the microfibrils are arranged helically about the fiber longitudinal axis.[3] The S_2 layer is the thickest of the three sublayers, contains the most cellulose[1,3] and is considered to be the component of the fiber that dictates its mechanical properties.[2,4] The primary load-bearing component of the fiber is the cellulose within the S_2 layer.[2,5] Therefore, the fundamental deformation behavior of paper should show similarities to the behavior of cellulose. The hemicelluloses and lignin can modify this behavior, as they are the material surrounding the cellulose microfibrils and act to distribute load.

Correspondence to: T. Patterson (tim.patterson@ipst.gatech.edu).

Contract grant sponsor: IPST at Georgia Tech.

Paper is considered to be, along with other polymeric materials, a viscoelastic material.[6–9] When a stress is applied to a viscoelastic material, it will exhibit a combination of elastic strain (recoverable and time independent), viscous strain (permanent and time dependent), and delayed elastic strain (recoverable and time dependent).[6,7,9,10] Viscoelastic polymeric materials exhibit creep behavior which is characterized as a time-dependent deformation (strain) upon application of a constant stress.[6,7,9,10] As the applied stress is increased, so does the amount of creep. Most creep testing is conducted under a constant load, which is considered to be a close approximation of constant stress under low strains.[6] However, stress does change during straining if a constant load is applied. Therefore, initial applied stress is often used to describe the creep behavior of a material when testing is conducted under a constant load.

In polymeric materials total creep strain can be broken down into a number of strain components; initial elastic strain, primary creep, and secondary creep. These terms are often used to describe creep behavior in metals where initial elastic strain is the ''instantaneous'' strain that occurs during initial loading, primary creep is characterized by a creep rate that is a function of time and decreases as time increases, and secondary creep is characterized by a creep rate that is independent (or nearly independent) of time.[6,11] Initial elastic strain and primary creep are considered to be fully recoverable while secondary creep is nonrecoverable.[6,11] When considering a polymeric material, Coffin[11] pointed out that secondary creep is not independent of time in tension, but is rather a function of time where creep rate decreases as time increases. As a result, primary creep and secondary creep in polymeric materials can only be differentiated by their recoverability, where primary creep is recoverable and secondary creep is nonrecoverable.

There also exists a component of creep called tertiary creep which occurs as a material approaches failure and is characterized by a dramatic increase in creep rate. As discussed by Coffin,[11] paper exhibits only a negligible amount of tertiary creep. Data from the work presented here supports this assumption. Figure 1 shows results where a 75% tensile strength load was applied to highly wet pressed (high density) paper made from bleached Kraft spruce and lodgepole pine fibers refined to 400 CSF mL freeness. This case showed the greatest amount of tertiary creep of all the sheets tested, yet total tertiary creep was less than 1% of the total strain and did not occur until close to failure, where the sheet structure is significantly compromised. Tertiary creep is not considered in the proposed model.

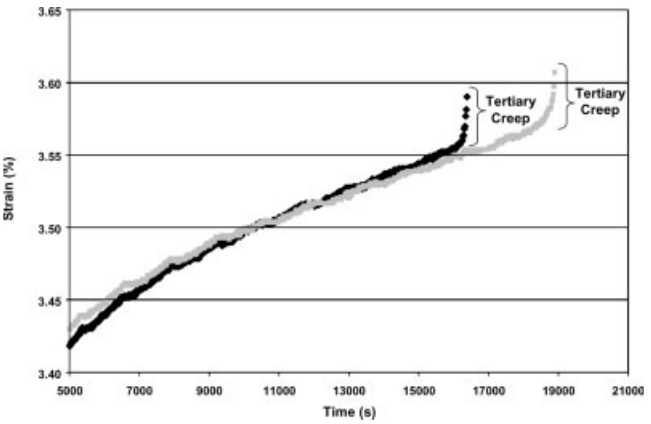

Figure 1 Tertiary creep in a highly wet pressed paper made from bleached Kraft spruce and lodgepole pine fiber refined to a 400 mL freeness.

In a previous work by DeMaio and Patterson,[12] it was found that as paper reaches higher levels of bonding, (i.e., the product of relative bonded area and specific bond strength) the bonding attains a level where fiber deformation is the only factor controlling paper creep deformation behavior. This occurs because a sufficient amount of bonding exists within the paper structure to effectively and evenly distribute load throughout the fiber network. This is considered to be a fully efficient loaded structure. At that point, any further increases in bonding will no longer affect creep behavior and only serve to increase the ultimate strength of the paper.

It was shown that efficiency factors can be used to account for the influence of bonding on creep behavior when the level of bonding is less than fully efficient. The efficiency factor is calculated by dividing the inefficient loaded structure elastic modulus by the fully efficient loaded structure elastic modulus. DeMaio and Patterson[12] used both 1955 creep data from Brezinski[13,14] and their own data to demonstrate that efficiency factors, calculated using elastic modulus data, were effective in accounting for the influence of bonding in creep behavior. Creep behavior of inefficiently loaded structures, presented using isochronous stress–strain curves, was shown to superimpose with creep behavior of fully efficient loaded structures, when efficiency factors were applied to account for bonding. Seth and Page[15] were previously able to show that efficiency factors could be used to account for bonding in stress–strain behavior (short time duration behavior).

The model presented within this article predicts creep strain in the form of isochronous stress–strain curves. These curves are generated by plotting total strain versus the initial applied stress at various snapshots in time. Panek et al.[16] and Soremark et al.[17] considered the use of isochronous stress–

strain curves as an effective way to analyze, simplify, and present creep data in paper and refer to others who have effectively used these curves to predict creep in other polymers. Temperature and moisture are not variables considered within this article, although future work could be done to incorporate them.

METHODS AND MATERIALS

Pulp and preparation

NIST standard reference material 8495 Northern Softwood Bleached Kraft Pulp was used in this study. The pulp arrived in dry lap sheets in a hermitically sealed packages. The pulp had remained sealed for approximately 15 years. The pulp was refined in a Valley Beater at a charge of 300 O.D. grams per batch. Refining time was varied so the final pulp Canadian Standard Freeness was either 570 or 400 mL. The pulp was prepared in such a manner to create straight, conformable fibers that would easily bond. Prior to making handsheets, the pulp slurry was treated with either a debonder or a bonder or received no treatment. The debonder used was a cationic surfactant (Incrosoft AS-55), from Croda, while the bonder used was locust bean gum, from σ-Aldrich. Bonder and debonder were added to the pulp slurry and mixed for 1 min at dosages of 0.45 and 0.11% by weight, respectively.

Handsheets

Handsheets were made using a 210 mm^2 Williams handsheet mold. A 100 mesh screen was used as the forming wire. The handsheets made from the treated pulp slurries were targeted to have an oven dry basis weight of 90 g/m^2. Sheets were wet pressed at either 1.03, 0.17, or 0.07 MPa, depending on sample set. Sheets were pressed for 5 min, followed by a blotter change and pressed again at the same level for 2 min. Gloss plates were not used. Handsheets were dried on a drum dryer under full restraint at 0.14 MPa steam pressure for 5 min. All sheets were immediately bagged, then placed in a 23°C and 50% RH room for conditioning prior to testing. Wet pressing acts to consolidate the sheet, thereby altering the relative bonded area of the sheet along with the caliper and density. The sheets pressed at low loads had a lower relative bonded area than those pressed at high loads. Bonder and debonder increase or decrease the specific bond strength, respectively. Given equal relative bonded area and different specific bond strengths, overall bonding is altered.

Creep testing

To characterize the papers prior to creep testing, grammage, hard caliper, ultrasonic velocities and formation tests were conducted. Creep testing was conducted using the IPST tensile creep tester under a constant 23°C and 50% RH condition. Samples were cut into 170 mm × 25 mm wide strips, mounted and conditioned for 24 h at 23°C and 50% RH condition prior to application of load. The free length of the samples after mounting was 140 mm. A series of different magnitude dead loads (initial applied stress levels) were evaluated. Displacements and failure times were recorded using linear variable displacement transducers (LVDT sensors) with the output signals sent to a computer based data acquisition system.

TENSILE CREEP RHEOLOGICAL MODEL

Modeling introduction

There are a limited number of modeling examples that can be drawn upon with regard to tensile creep in paper. Brezinski[13,14] utilized simple exponential and logarithmic functions to describe the results from his work. He stated that at short times and low initial applied stress levels, creep behavior followed an exponential trend. At longer times and high initial applied stress levels, creep behavior followed a logarithmic trend. The work of Hill[18,19] with single fiber tensile creep utilized the same rationale, focusing on creep behavior following a logarithmic trend. While these models are simple, the drawback is that the constants used must be changed when initial applied stresses are changed.

The work of Pecht et al.[20] was based in part on that of Brezinski[13,14] but employed a more complex empirical equation to describe tensile creep rather than using an exponential function to model creep at low initial applied stresses or short times and a logarithmic function to model creep at high initial applied stresses or long times. Further work by Pecht and Johnson[21] expanded the initial model to take moisture changes into account. Panek et al.[16] also proposed an empirical equation. While this model was derived specifically to predict isochronous creep curves, the use of hyperbolic tangent functions makes it difficult to use the model to solve for strain. None of these models took bonding into account. As all of these models are empirical in nature they offer limited predictive insight into the creep behavior of paper.

Rheological modeling background

In terms of rheological modeling in paper, there is little information from which to draw. The work of

Mason[22] discussed using several types of rheological models to describe creep in paper, including the use of a Maxwell Model (spring in series with a dashpot), a Voigt Model (spring in parallel with a dashpot), and a Burgers Model (Maxwell Model in series with a Voigt Model). More recently, the work of Pommier et al.[23] used two Voigt Models in series with a Maxwell Model to describe creep behavior. These models used linear springs and linear dashpots and hence yield a relationship where stress and strain have a linear relationship. In paper, stress and strain have a nonlinear relationship and the use of a rheological model based on elements with linear behaviors has inherent limitations on its accuracy. In addition, if the secondary creep component of strain is represented by a single dashpot, the result is a time independent strain rate, which is not representative of tensile creep in paper.

To account for the nonlinear stress–strain relationship, Coffin[11] developed a nonlinear tensile creep model. While the Coffin model is empirical in nature, it does contain rheological elements; a spring element to represent initial elastic strain, a function similar to a Voigt Model to account for primary creep and a nonlinear dashpot to represent secondary creep. The nonlinear dashpot employs a logarithmic function which allowed secondary creep rate to decrease as time increased. In addition, Coffin[11] employed an efficiency factor in the model and showed that it provides a reasonable prediction of the creep data from Brezinski.[13,14]

Agbezuge[24] introduced a nonlinear rheological model to describe the stress–strain behavior of xerographic papers. He used a 3-parameter rheological model in which a linear spring is used in parallel with a linear spring and nonlinear Eyring dashpot in series. A drawback to using the model for predicting creep behavior is it does not have a secondary creep component and assumes full recovery of strain. Sedlachek[25] utilized the same approach as Agbezuge[24] and found that it was also effective in predicting the creep behavior of single fibers. Both of these authors draw from the work of Halsey et al.[26] who were responsible for one of the earliest uses of the Eyring dashpot. They developed a 3-parameter rheological model where a linear spring in parallel with a Maxwell Model was modified by replacing the linear (Newtonian) dashpot with a Eyring dashpot. Later Holland et al.[27] employed the same approach with the Burger's Model where both linear dashpots were replaced with Eyring dashpots. This 4-parameter model provided greater utility than the 3-parameter model as it separated initial elastic strain and primary creep as well as adding a secondary creep parameter.

The Eyring dashpot is a nonlinear dashpot that can be used to relate the creep deformation mechanism to potential (or reaction rate) theory. It is based on an Arrhenius reaction rate where constants incorporate temperature, energy of activation, volume of flowing (molecular) segments, and the volume of empty or vacated spaces. The dashpot was first introduced by Tobolsky and Eyring[28] in 1943. The theory behind the model states that in order for flow or strain to occur, a potential barrier must be overcome. The addition of stress acts to shift this barrier to where the energy required to overcome it becomes less in one direction causing a bias and allowing flow or strain in the direction of the bias to occur. Halsey et al.[26] and Holland et al.[27] applied the Eyring dashpot to polymeric materials that contained amorphous (disordered) regions within their molecular networks. In this article, the phrase 'molecular network' refers to the arrangement of the molecules that compose the polymer (i.e., the arrangement of the molecular network is amorphous, crystalline, or partially crystalline). As stated previously, the primary load bearing component in a papermaking fiber is cellulose, a partially crystalline linear chain molecule. The cellulose is contained in a matrix which incorporates two amorphous elements; hemicelluloses and lignin.[1,4,8] As a result, use of the Eyring dashpot is particularly applicable to the modeling of paper and papermaking fibers. In combination with linear (Hookean) spring elements in a rheological model, the Eyring dashpot can be used to suggest an explanation for creep deformation on a molecular level.

The previous work employing the Eyring dashpot did not take into account several factors which are important to the accurate modeling of tensile creep in paper. There was no direct means of taking into account the level of bonding, bonding was taken into account by altering the constants employed. Thus, any change in bonding required a recalculation of the model constants. Secondary creep rate was modeled as time independent, while it is actually time dependent. Consideration was not given to creep behavior at low initial applied stresses. These are stress levels that can be characterized as below the elastic limit on a stress–strain curve.

Rheological model derivation

The following derivation develops a nonlinear rheological model of creep behavior which employs linear Hookean springs and nonlinear Eyring dashpots. The model predicts strain as a function of initial applied stress, time and bonding level as described by bonding efficiency factor. It also separates the total creep strain into initial elastic strain, primary creep, and secondary creep components. The total strain from creep, ε, is the sum of ε_e, initial elastic

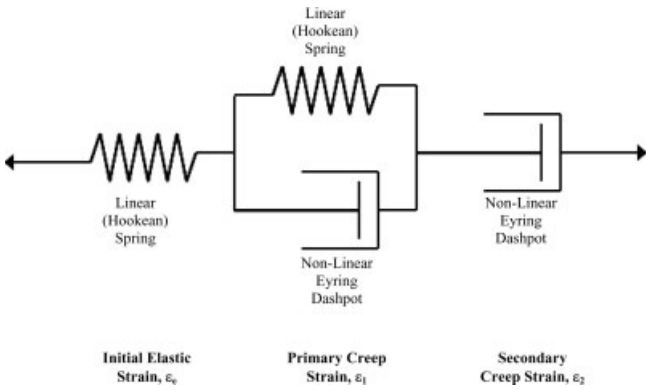

Figure 2 Four-parameter rheological model used to predict tensile creep behavior in paper.

strain, ε_1, primary creep strain, and ε_2, secondary creep strain. This is shown in eq. (1), where σ_o is the initial applied stress and t is time.

$$\varepsilon = \varepsilon_e(\sigma_o) + \varepsilon_1(\sigma_o, t) + \varepsilon_2(\sigma_o, t) \tag{1}$$

Initial elastic strain is only a function of the initial applied stress, whereas primary creep strain and secondary creep strain are functions of both initial applied stress and time. Drawing from the work of Holland et al.,[27] a two spring-two dashpot model was selected as a starting point to represent the strains in eq. (1). Figure 2 shows a representation of this model. Initial elastic strain is represented by a linear spring, primary creep strain is represented by a linear spring in parallel with a nonlinear Eyring dashpot, and secondary creep strain is represented by a nonlinear Eyring dashpot.

Equation 2 shows the relation for initial elastic strain, where initial elastic strain is represented by Hooke's Law.

$$\varepsilon_e = \frac{\sigma_o}{E_e} \tag{2}$$

In eq. (2), E_e, the elastic modulus of the paper relates initial applied stress to initial elastic strain. Initial elastic strain occurs immediately upon application of the stress to the paper. When this stress is removed, the strain will instantaneously and fully recover. If this deformation is thought of from a molecular standpoint, eq. (2) represents the initial elastic response of the cellulose chains and the molecular (partially crystalline) network of which they are composed. This is the same explanation put forth by Meredith,[29] when he referred to the elasticity associated with partially crystalline polymeric linear chain molecules.

Primary creep strain (recoverable strain) is represented by a linear spring in parallel with a nonlinear Eyring dashpot. When the spring and dashpot are connected in parallel, the strain and strain rate associated with each element are equivalent and represent the primary creep strain and primary creep strain rate respectively. Equation 3 shows the relation for the linear spring where σ_s is the stress on the spring, ε_1 is the primary creep strain, and E_1 is the spring constant.

$$\sigma_s = E_1\varepsilon_1 \tag{3}$$

Equation 4 shows the relation for the nonlinear Eyring dashpot where σ_d is stress on the dashpot, $d\varepsilon_1/dt$ is the strain rate of the dashpot, and A_1 and B_1 are the dashpot constants. The B_1 constant incorporates the effects of temperature, energy of activation, volume of flowing molecular segments, and the volume of empty or vacated spaces within a polymeric material. The A_1 constant includes temperature and the volume of empty or vacated spaces.

$$\sigma_d = A_1 \sinh^{-1}\left(\frac{1}{B_1}\frac{d\varepsilon_1}{dt}\right) \tag{4}$$

While the strain and strain rate associated with each element are the same when connected in parallel, the stresses are not; each element bears a different portion of the applied stress. As a result, initial applied stress is found when eqs. (3) and (4) are summed, yielding eq. (5) where initial applied stress, σ_o, is a function of primary creep strain and primary creep strain rate.

$$\sigma_o = E_1\varepsilon_1 + A_1 \sinh^{-1}\left(\frac{1}{B_1}\frac{d\varepsilon_1}{dt}\right) \tag{5}$$

Equation 5 must be rearranged and solved for strain in terms of stress. Equation 5 is first stated as

$$\frac{d\varepsilon_1}{dt} = B_1 \sinh\left(\frac{\sigma_o - E_1\varepsilon_1}{A_1}\right) \tag{6}$$

Equation 6 is solved, resulting in eq. (7) which shows primary creep strain as a function of initial applied stress and time where E_1, A_1, and B_1 are material constants.

$$\varepsilon_1 = \frac{1}{E_1}\left(\sigma_o - 2A_1 \tanh^{-1}\left[\tanh\left(\frac{\sigma_o}{2A_1}\right)\exp\left(-\frac{E_1B_1t}{A_1}\right)\right]\right) \tag{7}$$

By eq. (7), as time increases, the initial applied stress will be borne completely by the spring element. As a result, the total amount of primary creep strain will be linearly related to initial applied stress, given enough time. The constant, E_1 determines the total amount of primary creep strain that will occur for a given stress. The constants, A_1 and B_1 control the

delayed elastic behavior of the paper. Specifically, A_1 determines primary creep strain linearity with stress. B_1 determines the rate at which primary creep will progress and exhaust.

Meredith[29] stated primary creep behavior was the delayed elastic response of the amorphous molecular network with respect to polymeric materials. Alfrey[30] stated that primary creep was flow resulting from the uncurling of molecular chains within the amorphous regions of a polymer network. In terms of paper, primary creep strain would be the uncurling of the amorphous regions of the molecular network within cellulose chains. Uncurling of amorphous hemicelluloses and amorphous would also occur.

Secondary creep strain (permanent strain) is represented by a single nonlinear Eyring dashpot. Equation 8 shows the relation for a nonlinear Eyring dashpot where $d\varepsilon_2/dt$ is secondary creep strain rate, σ_o is initial applied stress and A_2 and B_2 are material constants.

$$\frac{d\varepsilon_2}{dt} = B_2 \sinh\left(\frac{\sigma_o}{A_2}\right) \tag{8}$$

Equation 8, when solved, yields a relationship in which secondary creep strain is nonlinear with initial applied stress and secondary creep strain is linear with time. However, secondary tensile creep strain in paper is not linear with time. As shown by Brezinski,[13,14] secondary creep strain in paper is linear with log time. To account for this, eq. (8) is modified to incorporate a time dependence on secondary creep strain rate. This is shown in eq. (9), where a time term, $(t/t_r + 1)$ is incorporated into the Eyring dashpot relation.

$$\frac{d\varepsilon_2}{dt} = \left[B_2 \sinh\left(\frac{\sigma_o}{A_2}\right)\right] \frac{1}{t/t_r + 1} \tag{9}$$

This approach, using a reference time, has been used previously in theoretical applications to elasto-visco-plastic constitutive equations,[31] creep in tubes,[32] creep in sand[33] as well as creep in paper.[16] When the differential equation in eq. (9) is integrated, eq. (10) results which shows secondary creep strain as a function of initial applied stress and time where A_2 and B_2 are material constants and t_r is a reference time constant. The reference time constant is determined by the time scale for which the creep measurements are made.

$$\varepsilon_2 = \left[B_2 \sinh\left(\frac{\sigma_o}{A_2}\right)\right] t_r \ln\left(\frac{t}{t_r} + 1\right) \tag{10}$$

According to eq. (10), as time increases, the rate of secondary creep will diminish. The constants, A_2 and B_2 represent the viscous behavior of the paper. A_2 determines the secondary creep strain linearity with stress and B_2 determines the rate at which secondary creep will progress. Within the Eyring dashpot, the B_2 constant includes the effects of temperature, energy of activation, volume of flowing (molecular segments), and the volume of empty or vacated spaces. The A_2 constant includes temperature and the volume of empty or vacated spaces. Unlike the primary creep strain case, if initial applied stress is removed, the secondary creep strain will not recover. Alfrey[30] stated secondary creep behavior as a permanent deformation involving the sliding of molecular segments past one another within the amorphous region of a molecular network. Tobolsky and Eyring[28] similarly stated the flow of molecular segments and the breaking of network bonds. In terms of paper, secondary creep strain would be the sliding of cellulose chain segments past one another within the amorphous regions of the molecular network within the fiber. The flow of amorphous hemicelluloses segments and lignin also contributes to the behavior.

The work of Olsson and Salmén[34] offer support to the rationale behind the molecular mechanisms being part of the explanation describing primary creep and secondary creep strain. Using mid-IR spectroscopy, Olsson and Salmén[34] found that there appeared to be an increase in orientation (alignment towards the direction of the applied stress) or stretching of cellulose molecules and the indication of sliding between cellulose chains. Although they did not attribute these observations specifically to primary creep strain and secondary creep strain, increase of orientation could be attributed to primary creep strain and sliding of molecular chains could be attributed to secondary creep strain. This would be consistent with what Alfrey[30] stated as the mechanisms behind primary and secondary creep strain.

Equations 2, 7, and 10 are incorporated into eq. (1) to yield a rheological model which predicts total strain from creep as the sum of initial elastic strain, primary creep strain, and secondary creep strain. This is shown in eq. (11).

$$\varepsilon = \frac{\sigma_o}{E_e} + \frac{1}{E_1}\left(\sigma_o - 2A_1 \tanh^{-1}\left[\tanh\left(\frac{\sigma_o}{2A_1}\right) \times \exp\left(-\frac{E_1 B_1 t}{A_1}\right)\right]\right) + \left[B_2 \sinh\left(\frac{\sigma_o}{A_2}\right)\right] t_r \ln\left(\frac{t}{t_r} + 1\right) \tag{11}$$

However, eq. (11) does not adequately account for creep behavior at low initial applied stresses, stresses below the elastic limit on a stress–strain curve. To resolve this, prior research into stress relaxation behavior in paper can be drawn upon. Johanson and Kubat[35] researched stress relaxation behavior in paper and found that it is possible for paper to bear a

nonzero stress (now known as Kubat stress) without measurable relaxation. This suggested the possible existence of an activation stress for nonelastic, stress relaxation behavior. They proposed that the rate of stress relaxation becomes zero at or below this stress. As a result, Skowronski and Szwarcsztajn[36] concluded that paper would only react elastically below the Kubat stress. Similarly, Waterhouse[37] and Niskanen[38] stated that the Kubat stress must be overcome for any significant stress relaxation to occur. Niskanen[35] further discussed that stress relaxation may occur below the Kubat stress, but it is too slow to measure. Htun and de Ruvo[39,40] and Htun[41] found that Kubat stress existed in paper that was dried under restraint and that this stress correlates to the (drying) stress generated within paper during restrained drying. In effect, the restrained drying process acts to harden the material so a threshold stress, or activation stress, must be exceeded for any significant time-dependent behavior to occur. Conversely, if paper is freely dried, the Kubat stress will be zero as no material hardening occurs. Given that stress relaxation and creep are effectively the inverse of one another, it is proposed that if such an activation stress exists for stress relaxation behavior, that it would also exist for creep behavior. Like Niskanen,[38] it is not argued that time-dependent deformation ceases to occur below such an activation stress, but a change in deformation behavior occurs near this stress and all deformation below it can be ignored. As a result, an activation stress, σ_k, is incorporated in to eq. (11), resulting in eq. (12).

$$\varepsilon=\frac{\sigma_o}{E_e}+\frac{1}{E_1}\left(\langle\sigma_o-\sigma_k\rangle-2A_1\tanh^{-1}\left[\tanh\left(\frac{\langle\sigma_o-\sigma_k\rangle}{2A_1}\right)\times\exp\left(-\frac{E_1B_1t}{A_1}\right)\right]\right)+\left[B_2\sinh\left(\frac{\langle\sigma_o-\sigma_k\rangle}{A_2}\right)\right]t_r\times\ln\left(\frac{t}{t_r}+1\right)\quad(12)$$

As shown in eq. (12), an activation stress is incorporated into the time-dependent components of the model (primary and secondary creep strain equations). Specifically, activation stress is subtracted from initial applied stress and placed within McCauley Brackets (values within these brackets less than zero are equal to zero). While this behavior could be described using a Heaviside step function, McCauley Bracket's are often used when modeling material behavior which exhibits a step change, the most well known case being singularity functions used to describe the distribution of bending moments and shear stresses in Euler beams. As a result, if initial applied stress is less than the activation stress, only the initial elastic strain component of the rheological model will contribute towards the total strain during a creep test. Hence, the model will predict strain as only instantaneous linear elastic strain below the activation stress. If this deformation is thought of from a molecular standpoint, the molecular network in which cellulose chains and hemicelluloses are arranged within a fiber can support a finite amount of stress before significant time-dependent uncurling or viscous flow of molecular segments occurs.

The final step required to complete this rheological model is to incorporate the efficiency factor into eq. (12) by dividing the initial applied stress by the efficiency factor. The efficiency factor accounts for how changes in bonding reduce the initial applied stress necessary to achieve a given amount of strain in an inefficiently loaded structure. Equation 13 shows the final form of the rheological model, with efficiency factor, φ, incorporated into the model.

$$\varepsilon=\frac{\sigma_o}{\phi E_e}+\frac{1}{E_1}\left(\left\langle\frac{\sigma_o}{\phi}-\sigma_k\right\rangle-2A_1\tanh^{-1}\left[\tanh\left(\left\langle\frac{\sigma_o}{\phi}-\sigma_k\right\rangle\frac{1}{2A_1}\right)\exp\left(-\frac{E_1B_1t}{A_1}\right)\right]\right)+\left[B_2\sinh\left(\left\langle\frac{\sigma_o}{\phi}-\sigma_k\right\rangle\frac{1}{A_2}\right)\right]t_r\ln(t+1)\quad(13)$$

This rheological model is well suited for predicting isochronous stress–strain curves. It has three input variables, initial applied stress, time or loading duration, and efficiency factor. It contains a reference time constant that is defined by the time scale of the creep measurements. It also contains seven material constants, which are found by comparison with a single set of experimental data. It separates strain into its initial elastic, primary creep, and secondary creep components and also draws from the molecular deformation mechanisms of the partially crystalline cellulose chains, amorphous hemicelluloses, and lignin that compose a papermaking fiber. The values of the material constants used will also be influenced by fiber type, fiber defects, formation, and orientation.

Rheological model validation

To validate the rheological model shown in eq. (13), it is compared to creep results obtained experimentally at varying sheet structure efficiencies (levels of bonding). These include the experimental results presented by DeMaio and Patterson[12] and the experimental results of Brezinski.[13,14] First, a single set of experimental results from DeMaio and Patterson[12] are used to determine the seven model constants. Using these constants the model creep prediction for two other experimental cases is then compared to the experimental data for those cases.

This was accomplished by fitting the constants to the modulus and creep data from the 400 mL freeness (Bleached Kraft spruce and lodgepole pine fibers), 1.03 MPa wet pressed, bonder treated sheets of DeMaio and Patterson.[12] These sheets are fully efficient loaded structures (efficiency factor equal to 1.00), indicating bonding does not impact deformation behavior. The seven material constants, σ_k, E_e, E_1, A_1, B_1, A_2, and B_2 were selected to ''fit'' the model to these experimental results and remain unchanged when the model is used to predict creep behavior for two additional experimental cases with different initial applied stresses, times, and bonding efficiency factors.

The activation stress, σ_k, was determined experimentally by finding the initial applied stress at which creep became insignificant. Activation stress can more accurately be found by measuring the drying stress of the paper; drying stress and activation stress are equivalent. Elastic modulus, E_e, was also determined experimentally by measuring the elastic modulus of the paper using ultrasonic measuring techniques. To determine the values of the remaining constants, the amount of primary creep and secondary creep must be found. Without recovery data, which was not available with these experimental data, it was assumed that all the strain occurring after 10,000 s was secondary creep. This assumption is supported by earlier work of Brezinski[13,14] in which primary creep was complete in less than 10,000 s. The model developed here is later shown to accurately fit both the Brezinski[13,14] results (in which primary creep is determined by experiment) and results for the less than fully efficient sheets used in this study (in which the magnitude of primary creep is calculated). Using this assumption, A_2 and B_2 were found through an iterative process and these constants were adjusted until the residual difference between the actual secondary creep data and the values the rheological model predicted was minimized. By subtracting the secondary creep and instantaneous elastic strain from the total strain, the total amount of primary creep was found and used to set the E_1 constant. A_1 and B_1 were then found through an iterative process and these constants were adjusted until the residual difference between the actual primary creep data and the values the rheological model predicted was minimized. The reference time constant was set at 1 s as the experimental results obtained by DeMaio and Patterson[12] were obtained in a seconds time scale. Table I shows the values and units for these constants. Notice that the units for A_1 and B_1 (and A_2 and B_2) are such that their quotient results in the units of viscosity. This is not a coincidence; the relationship is commented on by Drosdov[10] when a rheological model incorporating an Eyring dashpot is simplified to a linear model.

TABLE I
Values of Rheological Model Constants Used to Fit Experimental Results of DeMaio and Patterson

Rheological model constants	Values	Units
σ_k	1.5	N/mm
E_e	960	N/mm
E_1	270	N/mm
A_1	0.085	N/mm
B_1	2.5E−08	1/s
A_2	4.6	N/mm
B_2	8.1E−04	1/s
t_r	1.0	s

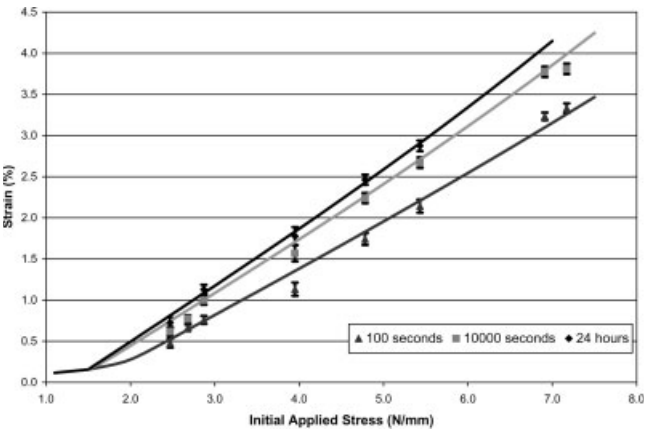

Figure 3 Isochronous stress–strain curves for 400 mL freeness, 1.03 MPa wet pressed, bonder treated sheets at 100, 10,000 s, and 24 h using the rheological model and an efficiency factor of 1.00.

Figure 3 shows isochronous stress–strain curves calculated using the rheological model in eq. (13) and the constants from Table I. Data points (with standard error bars) from the actual experimental creep results obtained from the 400 mL freeness, 1.03 MPa wet pressed, bonder treated, fully efficient sheets are also shown. As indicated by the Figure, the model fits well with the experimental results at all three times shown. Predictions from this model were then made for creep results from less than fully efficient loaded structures (i.e., sheets made from the same fibers as those used for the case shown in Figure 3, but prepared in such a way as to produce efficiency factors of less than one). Figures 4 and 5 illustrate isochronous stress–strain curves calculated using the rheological model in eq. (13) and the constants from Table I (i.e., the constants found using the data presented in Fig. 3). Data points (with standard error bars) from actual creep results obtained through experimentation are also shown. Figure 4 data was obtained from 400 mL freeness, 0.17 MPa wet pressed, debonder treated sheets with

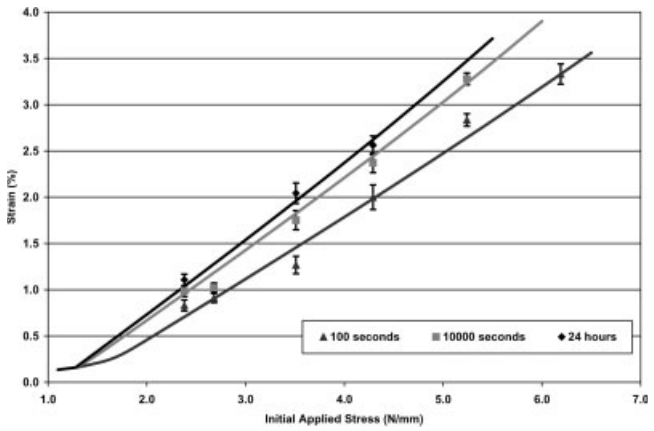

Figure 4 Isochronous stress–strain curves for 400 mL freeness, 0.17 MPa wet pressed, debonder treated sheets at 100, 10,000 s and 24 h using the rheological model and an efficiency factor of 0.85.

0.85 efficiency factors. Figure 5 data was obtained from 570 mL freeness, 0.07 MPa wet pressed, control sheets with 0.62 efficiency factors. Note, these sheet types are different from each other and both sheet types are different from the sheet type referenced in Figure 3, the sheet type used to determine the seven material constants. All three sheet types showed different creep behaviors. As shown in Figures 4 and 5, the model correlates well to the experimental results of the inefficiently loaded sheets. This shows the rheological model, with an incorporated efficiency factor, correctly accounts for the influence of bonding on creep deformation.

Turning to the experimental creep results of Brezinski[13,14] from 1955, further validation of the rheological model is made. Once again, the seven material constants, σ_k, E_e, E_1, A_1, B_1, A_2, and B_2 are used to ''fit'' the model to a single set of experimental

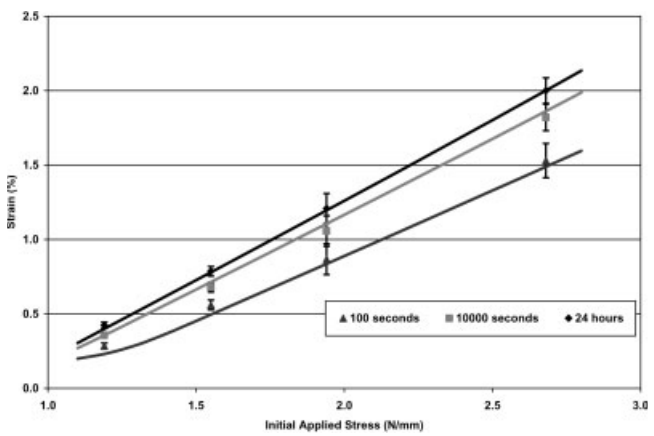

Figure 5 Isochronous stress–strain curves for 570 mL freeness, 0.07 MPa wet pressed, control sheets at 100, 10,000 s, and 24 h using the rheological model and an efficiency factor of 0.62.

results (creep data from the 425 mL freeness, 0.34 MPa wet pressed sheets, efficiency factor of 1.00, from Brezinski[13,14]) and remain unchanged when the model is used to predict behavior for two cases with different initial applied stresses, times, and efficiency factors.

All the material constants for this data were found in the same fashion as with the experimental results from DeMaio and Patterson.[12] The only exception is that actual creep recovery data was used to determine the amount of primary creep and secondary creep. As a result, the amount of primary creep and the E_1 constant did not have to be determined by subtracting the secondary creep and instantaneous elastic strain from the total strain. Instead, the primary creep was set at the amount of creep recovery and the secondary creep was set at the amount of nonrecovered creep. The secondary creep curve (used to iteratively solve for A_2 and B_2) was backed out by subtracting the creep recovery data. This was possible because the recovery test occurred under the same time duration as the creep test. The reference time constant was set at 1 s as the experimental results are in a seconds time scale. Table II shows the values and units for these constants.

Comparing the Brezinski[13,14] model constants to that of DeMaio and Patterson[12] the creep behavior measured by Brezinski has a lower activation stress, σ_k, more instantaneous elastic strain and secondary creep, and less primary creep compared to the experimental results of DeMaio and Patterson. Furthermore the constants indicate the creep behavior of Brezinski shows a more linear primary creep and less linear secondary creep than the experimental results of DeMaio and Patterson. A greater instantaneous elastic strain is indicated by the decreased elastic modulus, E_e. A lesser primary creep is indicated by a higher E_1 constant. With regard to the A_1 and B_1 constants, A_1 is higher in the Brezinski data, indicating a primary creep rate that is more linear with initial applied stress. B_1 is lower, indicating a slower rate at which primary creep will progress and eventually exhaust. Greater secondary creep is

TABLE II
Values of Rheological Model Constants Used to Fit Experimental Results of Brezinski

Rheological model constants	Values	Units
σ_k	0.9	N/mm
E_e	440	N/mm
E_1	360	N/mm
A_1	0.22	N/mm
B_1	1.3E−08	1/s
A_2	0.71	N/mm
B_2	3.9E−04	1/s
t_r	1.0	s

indicated by the A_2 and B_2 constants. A_2 is lower in the Brezinski data, indicating a more nonlinear secondary creep behavior. In fact, A_2 is significantly lower than the A_2 constant found for the experimental results from DeMaio and Patterson.[12] Because of this, B_2 is also lower, indicating at first glance a lesser secondary creep rate. This is not so because the decreased A_2 lessens the value of B_2 required to give a faster secondary creep rate. The reason this occurs is because A_2 and B_2 both share dependence on common parameters. These include the volume of the empty or vacated spaces within the molecular network of the fibers and temperature. This is also true for A_1 and B_1, but in this case, the differences in the primary creep rates were so large, the greater A_1 did not cause the value of B_1 to be higher than the B_1 constant used for the experimental results from DeMaio and Patterson.[12] This is a testament to how different pulp sources and processing techniques can affect paper behavior and how this model can be used to differentiate behaviors such as this.

Figure 6 show isochronous stress–strain curves calculated using the rheological model in eq. (13) and the constants from Table II. Figures 7 and 8 show predictions of creep behavior based on the material constants found using the data in Figure 6. Data points from actual creep results obtained from Brezinski[13,14] are also shown in all three Figures. These results were obtained from sheets with a range of efficiencies. Figure 6 data was obtained from the 425 mL freeness, 0.34 MPa wet pressed, fully efficient sheets used to find the material constants. Figure 7 data was obtained from 620 mL freeness, 1.38 MPa wet pressed sheets with efficiency factors of 0.88. Finally, Figure 8 data was obtained from 775 mL freeness, 0.07 MPa wet pressed sheets with efficiency factors of 0.62. It is worth noting that

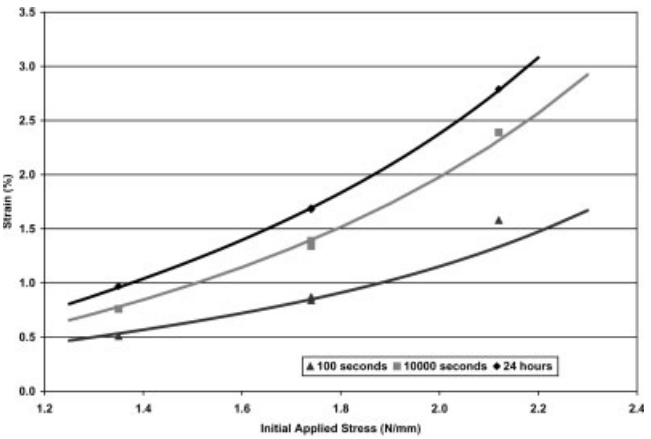

Figure 7 Isochronous stress–strain curves for 620 mL freeness, 1.38 MPa wet pressed sheets at 100, 10,000 s, and 24 h using the rheological model and an efficiency factor of 0.88.

Figures 3–5 present more or less linear isochronous results while Figures 6–8 present nonlinear isochronous results. The linear or nonlinear nature of the isochronous curves is dependent on the fiber type and sheet processing employed. These cases demonstrate that the model, without modification, is applicable to creep data which yields either linear or nonlinear isochronous creep curves.

The rheological model, demonstrates a behavior that is similar to an elastic-strain hardened response. The elastic strain-hardened response is present based in part on the introduction of an activation stress within the model. This causes the isochronous stress–strain curves to behave in a linear elastic manner below a certain initial applied stress. Almost 60 years ago, Steenberg[42] showed it possible for paper to have an elastic-strain hardened response in stress–strain curves. The model also allows the elas-

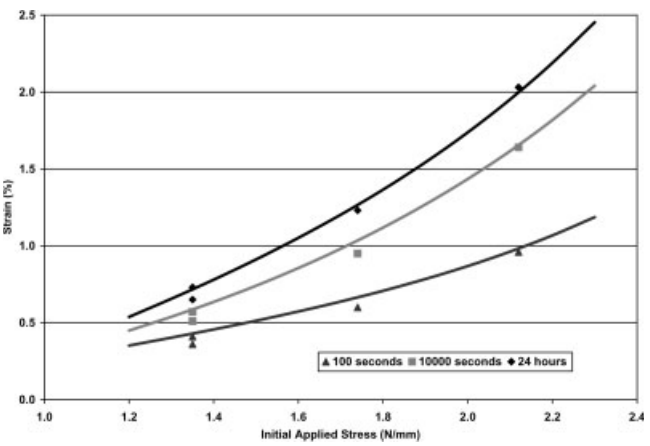

Figure 6 Isochronous stress–strain curves for 425 mL freeness, 0.34 MPa wet pressed sheets at 100, 10,000 s, and 24 h using the rheological model and an efficiency factor of 1.00.

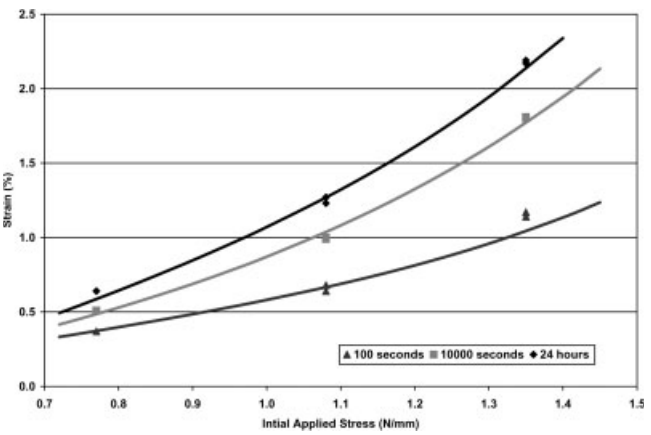

Figure 8 Isochronous stress–strain curves for 425 mL freeness, 0.07 MPa wet pressed sheets at 100, 10,000 s, and 24 h using the rheological model and an efficiency factor of 0.62.

tic limit to change as the time duration associated with the isochronous stress–strain curves is changed. At short times, the elastic limit is higher, and as time is increased, the elastic limit drops until it reaches the activation stress. The work of Johanson and Kubat[35] showed this type behavior with their stress–strain curve data. The behavior is also discussed by Skowronski and Szwarcsztajn.[36] In some cases, activation stress is zero because paper is freely dried or annealed. As a result, the elastic limit will go to zero as time is increased.

The main shortcoming of this model is it shows a tendency to under predict the strain at short times. The effect is amplified as the efficiency factor decreases. It will not be a good predictor of isochronous stress–strain curves when time is less than 10 s. This model does not take into account Brezinski's[13,14] observation, that creep strain in paper shows a power law dependence with time at low times. Therefore, a modification of the model would be necessary if curves at these short times were desired. This could be accomplished by making the secondary creep strain component of the model have a power law dependence with time instead of a logarithmic dependence.

CONCLUSIONS

The presented rheological model is a good predictor of isochronous stress–strain curves for the case of uni-axial tensile creep in paper. It uses initial applied stress, time, and efficiency factor as variables and separates creep into initial elastic, primary creep, and secondary creep components while drawing upon molecular deformation mechanisms. This rheological model is beneficial if a descriptive understanding of the total strain from creep or a specific contribution towards this strain is desired (for example, permanent strain associated with secondary creep). In addition, this model through comparison of constants would be useful in determining how fiber modifications, formation changes, orientation changes, etc., affect specific aspects of creep behavior.

This rheological model offers two powerful advantages toward predicting creep behavior. The first of these advantages is that since the constants in the models do not change, creep tests only need to be run for a short time to predict long-time isochronous stress–strain curves. With this model, the constants could be found in as little as 10,000 s or just less than 3 h. As a result, creep tests of under a day could be used to predict deformation over significantly longer periods of time. It is often impossible to conduct long-term creep tests with paper as temperature, humidity control, and intangibles can come into play. While not a requirement, if the model is to be utilized more effectively, creep recovery data should be available to easier separate the amounts of primary and secondary creep.

Second, and most importantly, this model is derived drawing upon the characteristics of the fibers with bonding influence being accounted for using an efficiency factor. This model draws from the deformation behavior of cellulose, hemicelluloses, lignin, and the molecular network associated with each of these fiber components. Interfiber bonds (relative bonded area and specific bond strength) are taken into account through the use of an efficiency factor which represents how effectively bonding is distributing load throughout the fiber network of the paper. As a result, these models make it possible to predict the creep behavior at a range of bonding levels; all that is needed is creep data from paper at one level of bonding. Then, using efficiency factors, the creep behavior of paper at any other level of bonding can be found. These efficiency factors can be found using ultrasonic velocity measurements. This will hold true as long as fibers (either type or amount of defects), formation, and orientation (both fiber and drying orientation) are not changed. This model confirms that bonding influence in paper can be accounted for with an easily derived efficiency factor.

Portions of the work were used by Mr. Andrew DeMaio as partial fulfillment of the requirements for the PhD program at the Georgia Institute of Technology.

References

1. Biermann, C. Handbook of Pulping and Papermaking; Academic Press: San Diego, CA, 1996.
2. Kortschot, M. In Fundamentals of Papermaking, Transactions of the 9th Fundamental Research Symposium; Baker, C., Ed.; FRC: Cambridge, UK, 1997; p 351.
3. Panshin, A.; De Zeeuw, C. Textbook of Wood Technology; McGraw-Hill: New York, NY, 1980.
4. Retulainen, E.; Niskanen, K.; Nilsen, N. In Paper Physics, Book 16; Niskanen, K., Ed.; Fapet Oy: Jyvaskyla, Finland, 1998; p 54.
5. Atalla, R. In Materials Interactions Relevant to the Pulp, Paper, and Wood Industries, Vol. 197; Caufield, D., Passaretti, J., Sobczynski, S., Eds.; Materials Research Society: Pittsburgh, PA, 1990; p 89.
6. Findley, W.; Lai, J.; Onaran, K. Creep and Relaxation of Nonlinear Viscoelastic Materials; Dover Publications: New York, 1989.
7. Malvern, L. Introduction to the Mechanics of a Continuous Medium; Prentice-Hall: Englewood Cliffs, NJ, 1969.
8. Waterhouse, J. In Pulp and Paper Manufacture, Vol. 9; Kouris, M., Ed.; Joint Textbook Committee of the Paper Industry: Atlanta, GA, 1992.
9. Young, R.; Lovell, P. Introduction to Polymers; Stanley Thornes Publishers: Cheltenham, UK, 1991.
10. Drozdov, A. Viscoelastic Structures; Academic Press: San Diego, CA, 1998.

11. Coffin, D. In Advance in Paper Science and Technology, Transactions of the 13th Fundamental Research Symposium; Anson, S. Ed.; FRC: Cambridge, UK, 2005; p 651.
12. DeMaio, A.; Patterson, T. In Advances in Paper Science and Technology, Transactions of the 13th Fundamental Research Symposium; Anson, S., Ed.; FRC: Cambridge, UK, 2005; p 749.
13. Brezinski, J. Tappi J 1956, 39, 116.
14. Brezinski, J. Ph.D. Dissertation, Institute of Paper Chemistry: Appleton, Wisconsin, 1955.
15. Seth, R.; Page, D. In The Role of Fundamental Research in Papermaking, Transactions of the 7th Fundamental Research Symposium; Brander, J., Ed.; FRC: Cambridge, UK, 1981; p 421.
16. Panek, J.; Fellers, C.; Haraldsson, T. Nordic Pulp Pap Res J 2004, 19, 155.
17. Soremark, C.; Fellers, C.; Henriksson, L. In Products of Papermaking, Transactions of the 10th Fundamental Research Symposium; Baker, C., Ed.; FRC: Oxford, UK, 1993; p 547.
18. Hill, R. Tappi J 1967, 50, 432.
19. Hill, R. Ph.D. Dissertation, Institute of Paper Chemistry: Appleton, Wisconsin, 1967.
20. Pecht, M.; Johnson, M.; Rowlands, R. Tappi J 1984, 67, 106.
21. Pecht, M.; Johnson, M. Tappi J 1985, 68, 90.
22. Mason, S. Pulp Pap Mag Can 1948, 49, 207.
23. Pommier, J.; Poustis, J.; Castets, C. The 1992 Progress in Paper Physics Seminar, Otaniemi, Finland 1992, p 59.
24. Agbezuge, L. Polym Eng Sci 1981, 21, 538.
25. Sedlachek, K. Ph.D. Dissertation, Institute of Paper Science and Technology: Atlanta, Georgia, 1995.
26. Halsey, G.; White, H.; Eyring, H. Text Res J 1945, 15, 295.
27. Holland, H.; Halsey, G.; Eyring, H. Text Res J 1946, 16, 201.
28. Tobolsky, A.; Eyring, H. J Chem Phys 1943, 11, 125.
29. Meredith, R. The Mechanical Properties of Textile Fibres; Interscience Publishers: New York, NY, 1956.
30. Alfrey, T. Mechanical Behavior of High Polymers; Interscience Publishers: New York, NY, 1948.
31. Gotch, M. Int J Non-linear Mech 1977, 12, 113.
32. Loghman, A.; Wahab, M. A. Int J Press Vessels Piping 1996, 67, 105.
33. Pestana, J. M.; Whittle, A. J Geotechn 48, 695.
34. Olsson, A.; Salmen, L. J Appl Polym Sci 2001, 79, 1590.
35. Johanson, F.; Kubat, J. Sven Papperstidning 1964, 67, 822.
36. Skowronski, J.; Szwarcsztajn, E. Przegl Papierniczy 1980, 36, 321.
37. Waterhouse, J. In Handbook of Physical Testing of Paper, Vol. 1; Mark, R.; Habeger, C.; Borch, J.; Lyne, M., Eds.; Marcel Dekker: New York, NY, 2002; p 527.
38. Niskanen, K. In Paper Physics, Book 16; Niskanen, K., Ed.; Fapet Oy: Jyvaskyla, Finland 1998; p 260.
39. Htun, M.; De Ruvo, A. Tappi J 1978, 61, 75.
40. Htun, M.; de Ruvo, A. In Fibre-Water Interactions in Papermaking, Transactions of the 6th Fundamental Research Symposium; Bolam, F.; Ed.; FRC: Oxford, UK 1977; p 477.
41. Htun, M. In Paper, Structure and Properties; Bristow, J; Kolseth, P., Eds.; Marcel Dekker: New York, NY, 1986; p 227.
42. Steenberg, B. Sven Papperstidning 1947, 50, 127.